Published in "The Plant Journal 80(5): 758–771, 2014"
which should be cited to refer to this work.

The inter-kingdom volatile signal indole promotes root development by interfering with auxin signalling

Aurélien Bailly[1,2,*], Ulrike Groenhagen[3], Stefan Schulz[3], Markus Geisler[4], Leo Eberl[1] and Laure Weisskopf[1,2,*]
[1]*Department of Microbiology, Institute of Plant Biology, University of Zurich, Zurich, Switzerland,*
[2]*Institute for Sustainability Sciences, Agroscope, Zurich, Switzerland,*
[3]*Institut für Organische Chemie, Technische Universität Braunschweig, Braunschweig, Germany, and*
[4]*Department of Biology – Plant Biology, University of Fribourg, Fribourg, Switzerland*

*For correspondence (e-mails aurelien.bailly@agroscope.admin.ch; laure.weisskopf@agroscope.admin.ch).

SUMMARY

Recently, emission of volatile organic compounds (VOCs) has emerged as a mode of communication between bacteria and plants. Although some bacterial VOCs that promote plant growth have been identified, their underlying mechanism of action is unknown. Here we demonstrate that indole, which was identified using a screen for Arabidopsis growth promotion by VOCs from soil-borne bacteria, is a potent plant-growth modulator. Its prominent role in increasing the plant secondary root network is mediated by interfering with the auxin-signalling machinery. Using auxin reporter lines and classic auxin physiological and transport assays we show that the indole signal invades the plant body, reaches zones of auxin activity and acts in a polar auxin transport-dependent bimodal mechanism to trigger differential cellular auxin responses. Our results suggest that indole, beyond its importance as a bacterial signal molecule, can serve as a remote messenger to manipulate plant growth and development.

Keywords: plant–microbe interaction, volatile organic compounds, auxin signalling, root development, *Arabidopsis thaliana*, *Escherichia coli*, plant-growth-promoting rhizobacteria.

http://doc.rero.ch

INTRODUCTION

The carbon-rich environment of the rhizosphere attracts and hosts a complex microbiome, distinct from bulk soil communities (Bais *et al.*, 2004; Bulgarelli *et al.*, 2012; Lundberg *et al.*, 2012). The root system therefore represents a dynamic environment where rapid and targeted communication between soil microbes and plants is an important asset for the survival of both partners. Plant beneficial bacteria and fungi have been described to promote plant growth and alter the root architecture of host plants (Contreras-Cornejo *et al.*, 2009; Felten *et al.*, 2009; Ortiz-Castro *et al.*, 2009; Bhattacharyya and Jha, 2012). In addition to diffusible substances, recent studies have demonstrated that bacterial emissions also trigger drastic growth changes in their host plants (Ryu *et al.*, 2003; Vespermann *et al.*, 2007; Blom *et al.*, 2011), by providing essential nutrients, by interfering with hormonal balance, sugar sensing or by triggering induced systemic resistance (Zhang *et al.*, 2007, 2008, 2009; Kwon *et al.*, 2010; Meldau *et al.*, 2013; Zamioudis *et al.*, 2013). Although recent work provided evidence that the auxin-signalling machinery plays a central role in this process (Ryu *et al.*, 2003; Zhang *et al.*, 2007; Zamioudis *et al.*, 2013), the mode of action of candidate molecules responsible for the observed effects is so far unknown.

In an effort to pinpoint the active compounds responsible for VOC-mediated plant-growth promotion, we previously analysed 42 soil-borne bacterial strains and identified indole as a potent candidate molecule (Blom *et al.*, 2011). In the last decade, indole has been increasingly recognized as a major bacterial signal involved in functions ranging from biofilm formation to virulence and antibiotic resistance (Wang *et al.*, 2001; Di Martino *et al.*, 2003; Chant and Summers, 2007; Lee *et al.*, 2007, 2010, 2013; Han *et al.*, 2011; Vega *et al.*, 2012) and was shown to also act as an inter-kingdom signal (Anyanful *et al.*, 2005; Wikoff *et al.*, 2009; Bansal *et al.*, 2010; Chimerel *et al.*, 2013), yet its impact on plant development has so far been overlooked.

Using isotopic labelling, we show that plants are able to convert bacterial indole to auxin and that the polar auxin

transport machinery (PAT) is essential to the observed indole-induced lateral root (LR) promotion. However, beyond its conversion into auxin, accumulation of indole putatively leads to the production of a signal antagonizing auxin responses at the SCF^{TIR1} signalling pathway level. Our work reveals an elegant mechanism by which soil-borne bacteria remotely manipulate post-embryonic root development.

RESULTS

Indole mimics bacterial VOCs effects in promoting LR formation and shoot growth

Environmental plant growth promoting rhizobacterial (PGPR) strains producing different amounts of indole in their respective volatile bouquets have been previously characterized *in vitro.* (Blom *et al.*, 2011). We monitored the growth of *Arabidopsis thaliana* seedlings in the continuous presence of VOCs emitted by indole-producing *Pseudomonas* and *Burkholderia* species and by the well-known indole-producer *E. coli* (Figure S1). Strains with the highest indole production rates increased both plant biomass and LR formation. However, components of the VOCs blends produced by *P. aeruginosa*, *P. chlororaphis* and *P. fluorescens* strains, such as hydrogen cyanide, had deleterious effects on plant growth, thus revealing the limitations of this comparative approach. In order to discriminate the effect of indole from other volatile blend components, we thus compared the growth of *A. thaliana* subjected to VOCs from an *E. coli* wild-type (wt) strain, producing great amounts of indole when grown on LB medium, to that of its isogenic *tnaA* mutant, which is devoid of tryptophanase activity and thus unable to produce indole (Figure 1a,c). The WT strain stimulated a nearly three-fold increase in both plant biomass and LR number but had minor effects on primary root growth or root hair density in mature root zones (Figure 1a). As expected, volatiles emitted by the *tnaA* mutant had a strongly reduced impact on the above-mentioned plant parameters, ruling out a major effect of carbon dioxide on growth promotion (Kai and Piechulla, 2009). Continuous supply of low concentrations of pure indole to the growth medium, or provided as a volatile, led to increased plant biomass and LR number without impacting root hair or primary root growth (Figure 1a,b). Remarkably, VOCs emitted by rhizobacterial *Pseudomonas* strains were recently shown to trigger similar responses in *Arabidopsis* (Zamioudis *et al.*, 2013). Yet, long-term exposure to high amounts of indole led to negative effects on plant growth and development (Blom *et al.*, 2011). To better understand the influence of indole on LR development, we monitored the well established DR5 reporter system activity (Dubrovsky *et al.*, 2008) in plants exposed to *E. coli* volatiles or to pure indole. In both conditions the formation of young lateral root primordia (LRP) increased compared with controls and to roots exposed to volatiles of the *tnaA* mutant (Figure 1d). These results are in agreement with a recent study (Zamioudis *et al.*, 2013). However, indole or wt *E. coli* VOCs treatments did not modify the natural left-right alternating LR formation pattern (De Smet *et al.*, 2007) and the formed LRPs eventually elongated to mature LRs. This suggests that indole affects the early LR development rather than reprogramming pericycle cell fate.

Indole-induced LR formation depends on, but does not affect, the polar auxin transport system

The polar, tightly controlled transport of auxin is recognized as an essential local signal for lateral root formation (Reed *et al.*, 1998; Casimiro *et al.*, 2001; Bhalerao *et al.*, 2002; De Smet *et al.*, 2007). Local application of indole-containing agarose beads directly above the primary root tip of 5-day-old seedlings promoted LR formation along the growing root axis and ultimately led to an increased biomass (Figure 2a). The fact that the effect was not restricted to the application site implies that the indole-induced signal can translocate across the plant. The auxin efflux inhibitor 1-*N*-naphtylphtalamic acid (NPA) prevents LR formation by blocking shoot-to-root auxin movements (Reed *et al.*, 1998; Casimiro *et al.*, 2001). Accordingly, local application of NPA below the root-shoot junction (RSJ) of 5-day-old seedlings prevented LR appearance from the growing primary root (Figure 2b). This inhibition could not be significantly released by local application of indole downstream from the NPA source, demonstrating that PAT is essential for indole-induced LR formation.

The shoot-derived auxin signal controls LR emergence and elongation, while auxin originating from the mature primary root primordium activates lateral root initiation (LRI) (Bhalerao *et al.*, 2002). To further dissect the mechanism by which indole interferes with the plant secondary root network, we decapitated shoots of 8-day-old seedlings to remove the principal source of acropetal auxin. As previously reported (Bhalerao *et al.*, 2002), shoot excision at this developmental stage did not alter LR appearance when compared with intact seedlings under control conditions but significantly reduced primary root growth (Figures 2c and S2). Continuous indole treatment of decapitated seedlings promoted the appearance of LRPs (Figure 2c), most of which were close to the root tip. These primordia rarely emerged or elongated (398.2 μm ± 188.7 SD at 100 μM) and failed to develop vascular tissues. Moreover, treatments with 100 μM indole repressed root tip growth (Figure S2) and initiated a LRP at 4.26 mm ± 1.05 SD from the root tip in 80% of the tested seedlings. Interestingly, this distance corresponds to a second peak in the basipetal auxin concentration gradient observed at this growth stage (Bhalerao *et al.*, 2002). To assess if indole would directly block auxin fluxes issued from the primary root meristem,

http://doc.rero.ch

http://doc.rero.ch

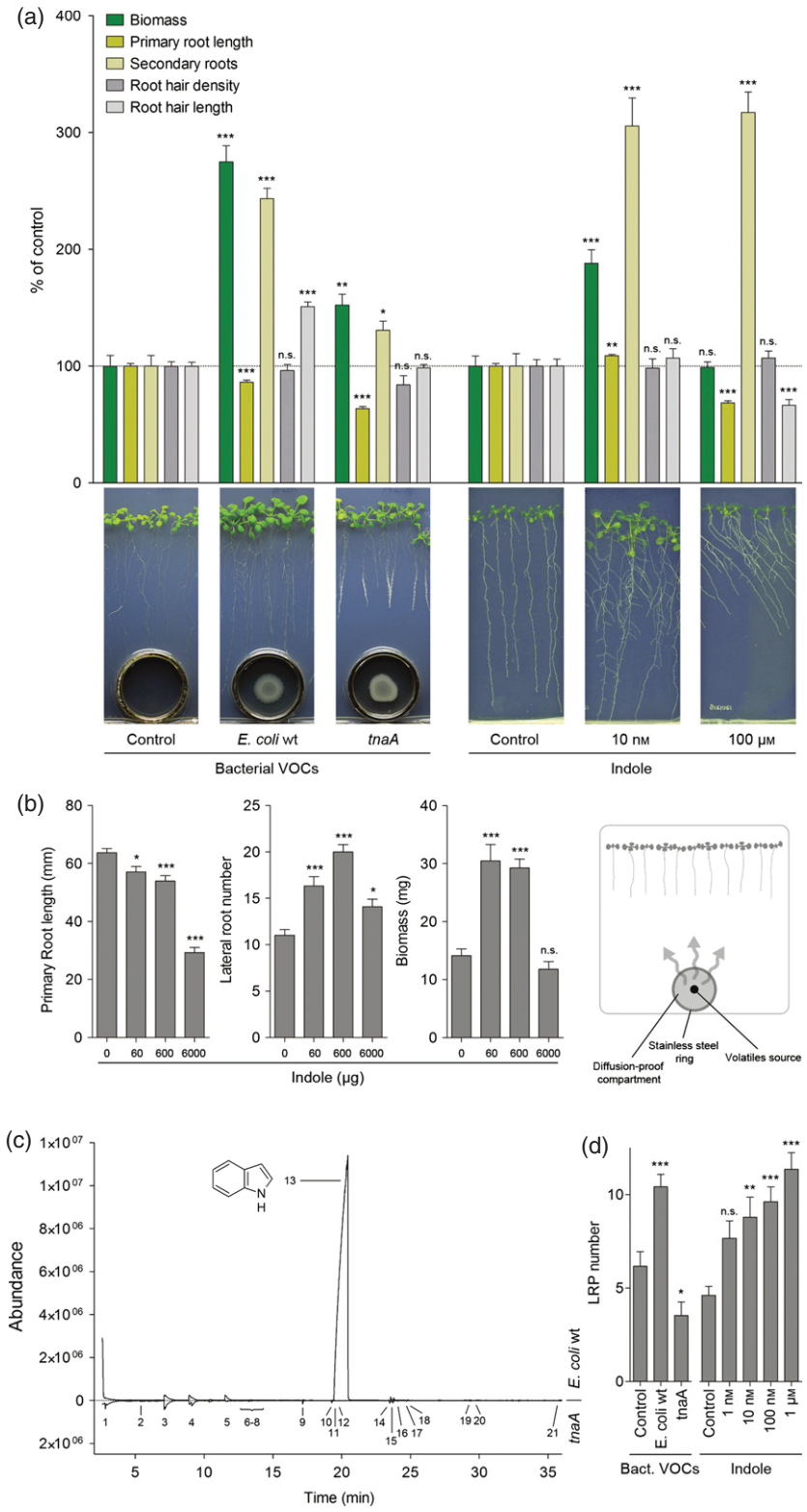

Figure 1. Bacterial volatile indole triggers increase in lateral root number and biomass in Arabidopsis.

(a) *Arabidopsis thaliana* seeds were co-cultured for 21 days after germination with wild-type *E. coli* or its *tnaA* mutant. Bacterial strains were physically separated from plants by a stainless iron ring in order to allow only gas exchange. In parallel, *A. thaliana* seedlings were germinated on growth medium supplemented with different concentrations of indole. Emerged lateral root numbers were scored after 14 days and shoots were excised after 21 days for biomass determination. Results shown are representative of biological triplicates and are expressed as mean ± standard error of the mean (SEM). Asterisks indicate statistical significance according to one-way analysis of variance (ANOVA) followed by Dunnet's post-hoc test ($n = 45$, $P < 0.001$).

(b) Seedlings were handled as described in Figure 1(a), except that indole was not directly supplied in the growth medium (left). Increasing amounts of indole were applied as a single 500-µl 1.25% agarose bead in the middle of the compartment defined by the stainless steel ring (see right scheme). Primary root length was measured and emerged lateral root numbers were counted after 14 days and shoots were excised after 21 days for biomass determination. Results shown are representative of biological duplicates and are expressed as mean ± SEM. Asterisks indicate statistical significance according to one-way ANOVA followed by Dunnet's post-hoc test ($n = 45$, $P < 0.001$).

(c) GC-MS spectra of headspace volatile organic compounds emitted by wild-type *E. coli* JM105 and its *tnaA* mutant grown on solid agar Luria-Bertani medium. Peak numbering refers to Table S1. Results shown are representative examples of two replicates of each strain.

(d) Non-emerged lateral root primordia were counted using the DR5 reporter system after 15 days of growth under constant exposure to bacterial VOCs or indole. Results shown are representative of biological duplicates and are expressed as mean ± SEM. Asterisks indicate statistical significance according to one-way ANOVA followed by Dunnet's post-hoc test ($n = 15$, $P < 0.001$). n.s., $P > 0.05$; $*P \leq 0.05$; $**P \leq 0.01$; $***P \leq 0.001$.

we next measured the basipetal transport of radiolabelled indole-3-acetic acid (IAA, the most abundant natural auxin) in intact seedlings. Basipetal auxin movements from the root tip or the hypocotyl were not significantly altered by 100 µM indole, suggesting no direct interference of indole or indole-derived metabolites with PAT (Figure 2d). These observations suggest that a proper, PAT-dependent indole signal is competent in initiating LR appearance.

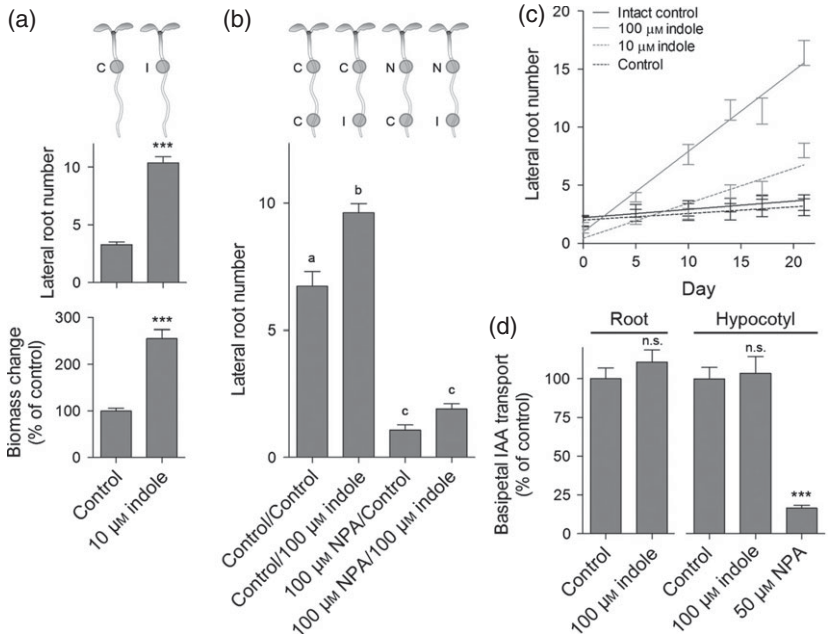

Figure 2. Indole-mediated lateral root promotion depends on polar auxin transport.
(a) Control (C) or indole-containing (I) agarose beads were applied below the root-shoot-junction of 5-day-old seedlings. Emerged lateral roots were scored and shoot fresh weights were determined after 8 and 16 days of treatment, respectively. Results shown are representative of biological triplicates and are expressed as mean ± standard error of the mean (SEM). Asterisks indicate statistical significance according to Student's *t*-test ($n = 12$, $P < 0.001$). n.s., not significant.
(b) Control (C), indole- (I) or NPA-containing (N) agarose beads were applied below the root-shoot-junction and above the primary root tip of 5-day-old seedlings. Lateral roots emerging along the growing primary root tip were scored after 8 days of treatment. Results shown are expressed as means ± SEM of biological duplicates. Letters indicate statistical significance according to one-way analysis of variance (ANOVA) followed by Tukey's post-hoc test ($n > 28$, $P < 0.001$).
(c) Eight-day-old control-germinated seedlings were transferred to fresh growth medium supplemented with indole or solvent and shoots were excised above the root-shoot-junction and kept in the dark. Lateral roots were continuously scored under the microscope. Results shown are representative of biological duplicates and expressed as mean ± SEM ($n = 24$).
(d) Agarose beads containing [^{3}H]-IAA and solvent or indole were placed over the primary root tip of 5-day-old seedlings transferred to fresh growth medium. After 16 h of transport the apical 3 mm of the root were excised and discarded and the amount of radioactivity in each subsequent 5 mm segment from the root tip was measured. Results shown are expressed as percentages of control treatments ± SEM of pooled biological triplicates. The amount of [^{3}H]-IAA transported into each segment for control and indole treatments was compared by Student's *t*-test and showed no statistically significant differences ($n = 12$).
n.s., not significant. $P > 0.05$; ***$P \leq 0.001$.

The mobile indole-induced signal is not transported through the polar auxin transport system

To verify the suggested mobility of indole, we applied radiolabeled indole at various positions along the root axis and imaged its movements in the plant body (Figure 3a). First, the radioactive signal appeared to travel at the same rates both basipetally and acropetally (Figures 3a and S3a). Thereafter, the signal accumulated in all meristematic tissues as well as at the RSJ. Finally, a strong signal was recorded in aerial tissues even when radioactive indole was applied to the distant root apex. Analogous results were obtained with a volatile source of radiolabelled indole (Figure S3b). We also measured basipetal indole transport from the root tip in consecutive root segments and found no competition with cold indole up to 1 mM, suggesting that indole or indole-derived metabolites movements do not depend on saturable transporters (Figure 3b). Additionally, 50-µM concentrations of the auxin efflux inhibitor, NPA, or of the auxin influx inhibitor 2-naphthoxyacetic acid (NOA) did not alter basipetal or acropetal indole transport (Figure 3c). We conclude that the indole signal is not transported through the PAT system and probably follows the vasculature streams.

Indole specifically affects auxin-controlled physiology

The observed indole accumulation led to alterations in auxin-controlled physiology beyond lateral root formation. Roots transferred to 10 µM indole displayed faster rates of curvature following gravistimulation compared with controls while roots exposed to 100 µM indole showed a decreased capacity to bend and were still responsive to NPA, indicating that indole interferes in a dose-dependent manner with the differential cell growth involved in root curvature (Figure 4a). In two different assays using photostimulated, etiolated seedlings, indole treatments resulted in a dose-dependent promotion of adventitious root number on intact hypocotyls (Figure 4b). The observed effect was much greater than with 1 µM exoge-

http://doc.rero.ch

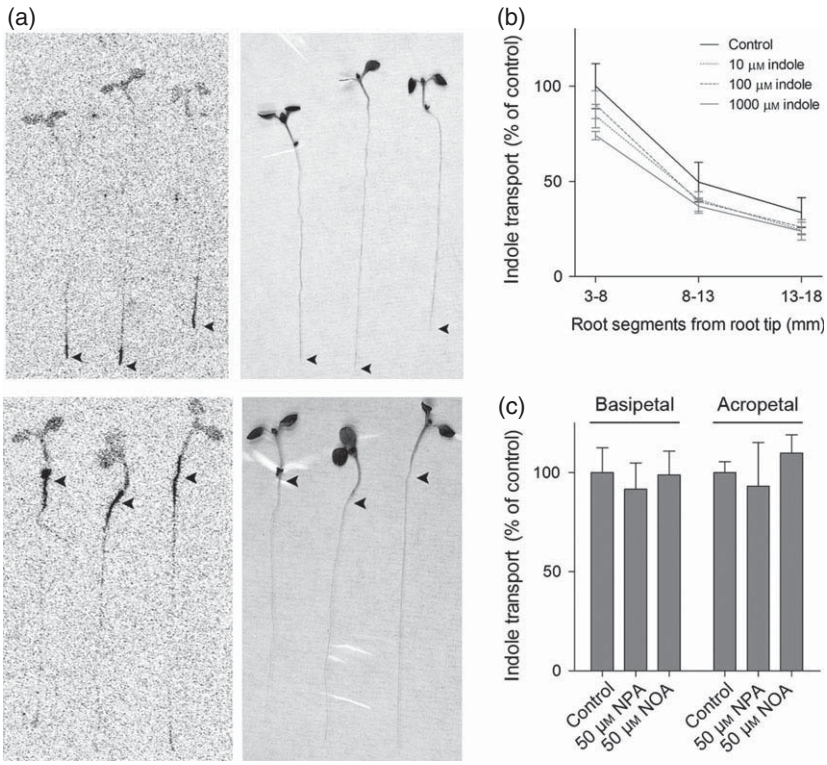

Figure 3. *In planta* indole movements are independent of the polar auxin transport system.
(a) Left, [^{14}C]-indole autoradiograms; right, corresponding seedlings after radiolabelling. Agarose beads containing [^{14}C]-indole were applied to either the primary root tip or root-shoot-junction of 7-day-old seedlings and autoradiograms were obtained after 16 h of treatment. Arrowheads indicate the position of the applied radioactive source.
(b) Indole homologous competition root basipetal transport assays. Results shown are expressed as percentages of control treatments ± standard error of the mean (SEM) of four pooled biological replicates. The amount of [^{14}C]-indole transported into each segment for control and cold indole treatments was compared by one-way analysis of variance (ANOVA) followed by Tukey's post-hoc test and showed no statistically significant differences (n = 12).
(c) Indole basipetal and acropetal transport in the root. Results shown are representative of biological triplicates and expressed as percentages of control treatments ± SEM. The amount of [^{14}C]-indole transported into each segment for control, NPA and NOA treatments was compared by one-way ANOVA followed by Dunnet's post-hoc test and showed no statistically significant differences (n = 4–6).

nous IAA when seedlings were returned to the dark after photostimulation. In the same extent, indole drastically increased adventitious root formation on hypocotyls exposed to the potent synthetic auxins 2,4-dichlorophenoxyacetic acid (2,4-D) and 1-naphthaleneacetic acid (NAA) (Figure S4a). Moreover, primary root growth inhibition occurred at a much higher IC_{50} dose for indole than for IAA treatments (125 μM versus 35 nM; Figure 4c). Etiolated seedlings grown on micromolar concentrations of indole showed a significant decrease in hypocotyl elongation without affecting gravitropic growth (Figure 4d). Furthermore, 100 μM indole treatments strongly promoted the auxin-controlled maintenance of the hypocotyl apical hook in etiolated seedlings (Figure 4d). Finally, control-germinated seedlings transferred to saturating exogenous IAA concentrations still responded to indole treatments in producing more and shorter LRs (Figure 4e). Similar indole-mediated differential effects were obtained against 2,4-D and NAA, but supplemental exogenous IAA treatments did not lead to comparable results (Figure S4b–d). In all these assays, the plants responded differently to high amounts of indole than they would to exogenous auxins or auxin transport inhibitors treatments (Schwark and Schierle, 1992; Lehman *et al.*, 1996; Yamamoto and Yamamoto, 1998; Ottenschlager *et al.*, 2003) and rather evoke the various effects reported for putative anti-auxins (Hayashi *et al.*, 2003, 2008, 2009; Oono *et al.*, 2003; Yamazoe *et al.*, 2005; Zhao and Hasenstein, 2010).

Continuous indole treatments trigger the DR5 auxin-responsive promoter

To verify the impact of indole on auxin perception, we quantified the fluorescent signal of the auxin-responsive *DR5::GFP* synthetic reporter (Ottenschlager *et al.*, 2003) under indole treatment. Germination and growth on 100 μM indole-supplemented medium led to enhanced GFP signal intensity in the root meristem restricted to the quiescent centre, columella initials and columella cell files as observed in control seedlings (Figure S5a). This increase in the GFP signal was not abolished by 20 μM NPA treatments and the presence of indole did not alter the NPA-induced signal expansion previously described (Ottenschlager *et al.*, 2003). Similar effects were observed at the RSJ (Figure S5b). This suggests that accumulation of indole may increase free IAA contents and/or alter its perception in these regions. Interestingly, an increase in the fluorescent signal was also observed in *DR5::vYFP*$_{NLS}$ seedlings exposed to *P. fluorescens* VOCs (Zamioudis *et al.*, 2013). We next transferred control- or indole-germinated *DR5::GUS* seedlings to fresh plates containing either 100 μM indole or 50 nM IAA and monitored the root β-glucuroni dase activity. Consistent with our *DR5::GFP* data, control-germinated seedlings transferred to indole displayed a GUS signal limited to the quiescent zones and columella compared with the control (Figure 5a). Germination on increasing indole concentrations resulted in a similar

http://doc.rero.ch

http://doc.rero.ch

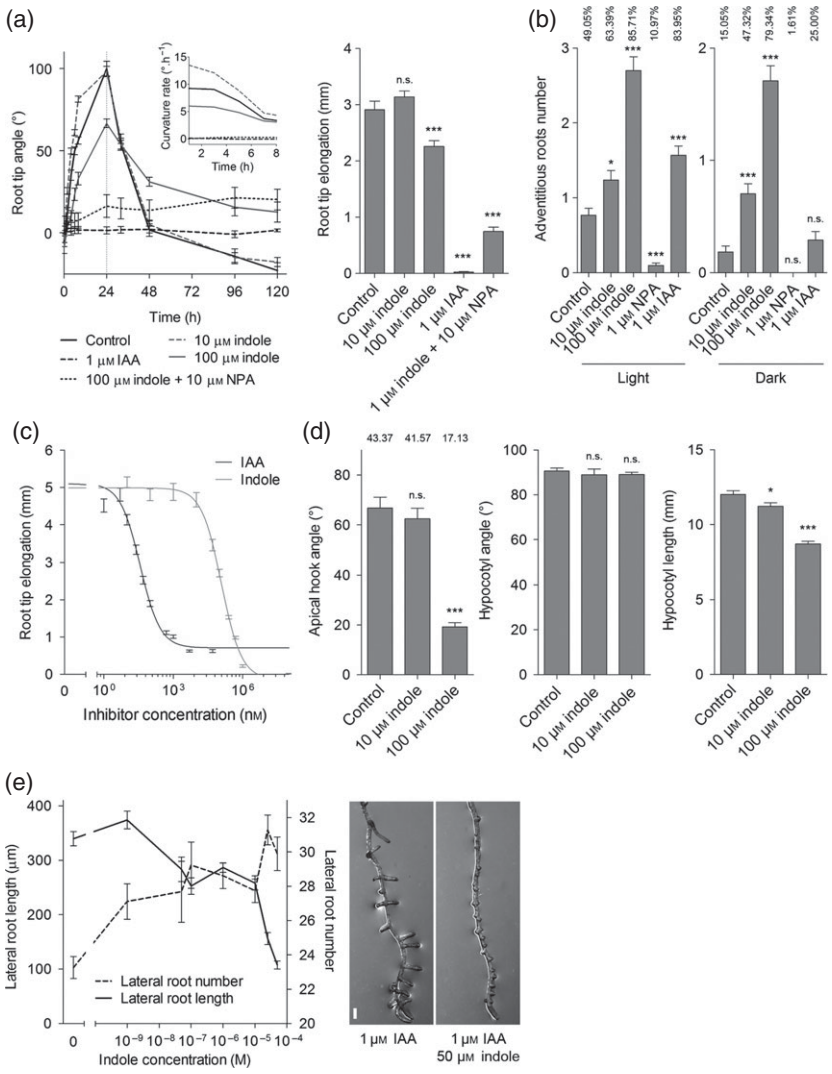

Figure 4. Indole alters auxin-controlled physiology.

(a) Left, gravitropic response and curvature rates of primary root tips of gravistimulated seedlings exposed to indole, IAA and NPA. Vertical dashed lines represent a second gravistimulation. Note that 10 µM indole treatment increased and 100 µM indole treatment decreased root bending capacity, but this inhibition was drastically different than in IAA treatment. Indole-treated roots still responded to NPA. Results shown are representative of biological duplicates and are expressed as mean ± SEM (n = 30). Right, primary root tip elongation of gravistimulated seedlings 24 h after stimulus. Results shown are representative of biological duplicates and are expressed as mean ± SEM. Asterisks indicate statistical significance according to one-way analysis of variance (ANOVA) followed by Dunnet's post-hoc test (n = 30, P < 0.001). n.s., not significant.

(b) Adventitious roots number appearing after photostimulation in subsequent light or dark growth conditions. Percentages above columns represent the proportions of seedlings developing at least one adventitious root on their hypocotyl. Results shown are representative of biological duplicates and are expressed as mean ± SEM. Asterisks indicate statistical significance according to one-way ANOVA followed by Dunnet's post-hoc test (n > 60, P < 0.001). n.s., not significant.

(c) Pharmacological impacts of indole and auxin on primary root tip elongation are dissimilar. Five-day-old control-germinated seedlings were transferred to fresh growth medium supplemented with increasing concentrations of indole or IAA and primary root tip extension was measured after 48 h. Results shown are representative of biological duplicates and are expressed as mean ± SEM. (n = 30).

(d) Hypocotyl physiology parameters of 5-day-old seedlings grown in dark conditions. Numbers above columns indicate the standard deviation. Results shown are representative of biological duplicates and are expressed as mean ± SEM. Asterisks indicate statistical significance according to one-way ANOVA followed by Dunnet's post-hoc test (n = 90, P < 0.001). n.s., not significant.

(e) Left, 5-day-old control-germinated seedlings were transferred to fresh growth medium supplemented with 1 µM IAA and increasing concentrations of indole. The number of lateral roots was counted and their lengths measured 5 days after treatment. Similar results were obtained with 5 and 10 µM IAA. Results are expressed as mean ± SEM. (n = 24–45). Right, Representative micrographs. Bar = 200 µm.

n.s., not significant. P > 0.05; *P ≤ 0.05; ***P ≤ 0.001.

signal pattern behaviour (Figure S6a,b). This spatial restriction was unexpected, as indole did not alter basipetal IAA transport (Figure 2d). Remarkably, *DR5::GUS* seedlings exposed to WT *E. coli* VOCs displayed the same signal pattern (Figure S6c) and a reduced GUS activity was measured in root tip tissues when compared with controls or

http://doc.rero.ch

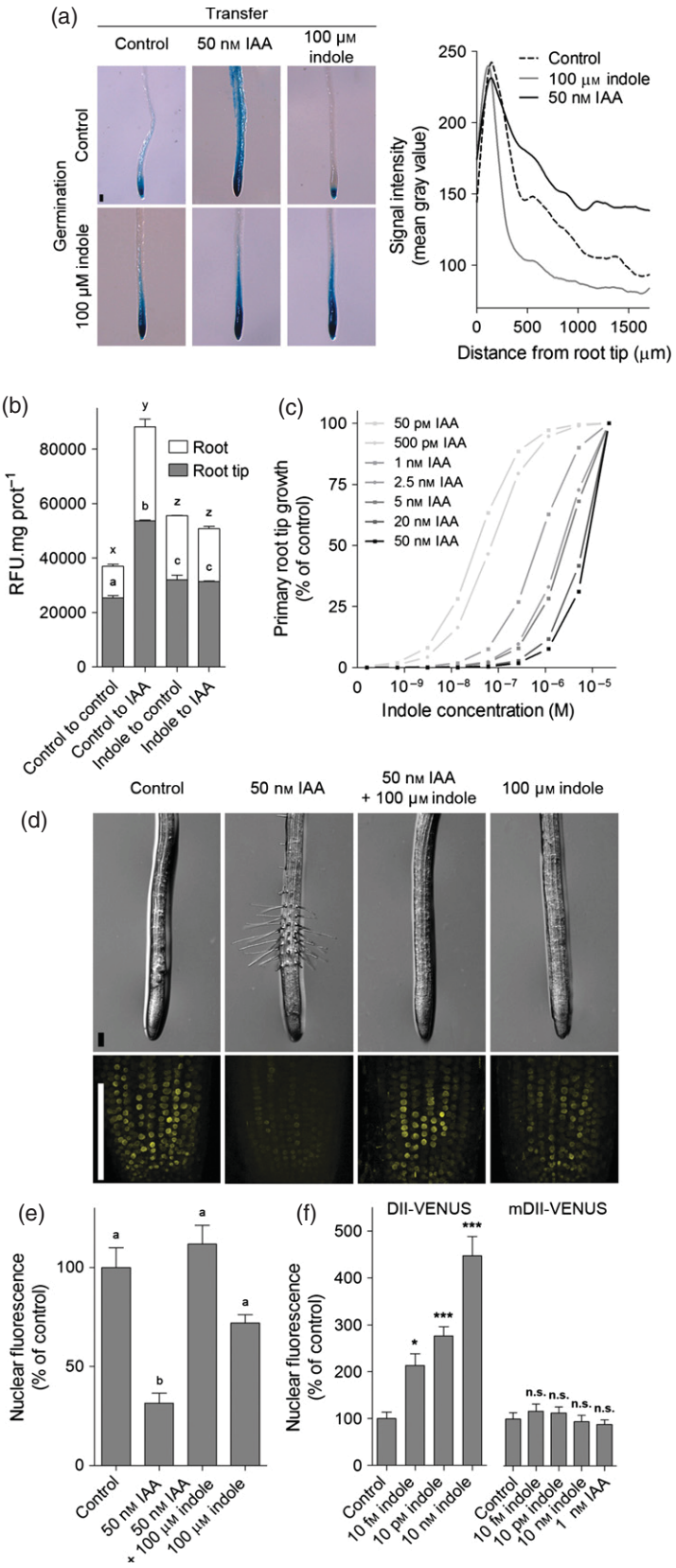

Figure 5. Indole accumulation alters auxin perception and signalling.

(a) Seven-day-old DR5::GUS seedlings germinated either on solvent control or indole-supplemented growth medium were transferred for 16 h onto fresh growth medium with indicated treatments. GUS activity was revealed after overnight histochemical staining (left) and the signal intensity along the longitudinal axis was measured (right). Results shown are representative of biological triplicates ($n = 30$). Bar = 100 µm.

(b) Enzymatic quantification of DR5 expression. DR5::GUS seedlings were handled as in Figure 4(a). Results shown are the means ± standard error of the mean (SEM) of biological triplicates ($n = 12$).

(c) Five-day-old control-germinated seedlings were transferred onto fresh growth medium supplemented with indicated IAA concentrations and solvent or increasing concentrations of indole. Primary root tip growth subsequent to transfer was measured 3 days after treatment and data were normalized. Results shown are expressed as mean ± SEM ($n > 24$).

(d) Seven-day-old control-germinated DII-VENUS seedlings were transferred for 16 h onto fresh growth medium supplemented with the indicated treatments. Seedlings were mounted in 10% glycerol. Results shown are maximum projections of 40 1.5-µm sections and are representative of biological triplicates ($n = 15$). Bars = 100 µm.

(e) Quantification of the nuclear VENUS fluorescent signal represented in Figure 4(d). Results shown are expressed as percentages of the integrated density of the fluorescence recorded in solvent control treatment conditions and are representative of biological triplicates. Letters indicate different statistical significance according to one-way analysis of variance (ANOVA) followed by Tukey's post-hoc test ($n = 15$, $P < 0.001$).

(f) Quantification of the nuclear DII-VENUS and mDII-VENUS fluorescent signals in 7-day-old seedlings geminated in the presence of indicated treatments. Results shown are expressed as percentages of the integrated density of the fluorescence recorded in solvent control treatment conditions and are representative of biological triplicates. Asterisks indicate statistical significance according to one-way ANOVA followed by Dunnet's post-hoc test ($n = 24$, $P < 0.001$).

n.s., not significant. $P > 0.05$; $^{*}P \leq 0.05$; $^{***}P \leq 0.001$.

to seedlings exposed to *tnaA* VOCs (Figure S6d). Such a decreased DR5 pattern has been previously reported in *Arabidopsis* seedlings in the presence of *Bacillus megaterium* (López-Bucio *et al.*, 2007), although the experimental setup did not allow ascribing this effect to VOCs only. In agreement with previous work (Ulmasov *et al.*, 1997), IAA treatment of control seedlings strongly promoted *DR5::GUS* expression in the whole root and root meristem (Figure 5a). Surprisingly, seedlings germinated on indole did not respond to the IAA stimulus, a phenotype reminiscent of that caused by putative anti-auxins (Hayashi *et al.*, 2003, 2009; Oono *et al.*, 2003; Yamazoe *et al.*, 2005). Enzymatic measurements confirmed these results and demonstrated that both root tips and mature roots had lost their ability to react to auxin (Figure 5b). Moreover, indole also impeded the DR5 response signal to the synthetic auxins 2,4-D and NAA both in intensity and distribution (Figure S4e).

Indole is partially converted into IAA via the tryptophan-dependant synthesis pathway

Several indole-induced physiological phenotypes together with the observed increase in DR5 promoter responses described above may simply be explained by mimicry of auxin action. As indole has been demonstrated to be an auxin synthesis precursor (Liu *et al.*, 2011), we measured free IAA levels in indole-treated plant tissues by gas chromatography–mass spectrometry. First, 5-day-old seedlings transferred for 24 h to 10 μM indole showed no significant accumulation of free IAA in their roots or shoots when compared with controls (Figure S7a). Next, increasing amounts of [^{13}C]indole were used to trace the potential conversion of the compound into IAA. We monitored a linear increase in [^{13}C]IAA in both shoots and roots, reaching a threefold enrichment in total free IAA in the 100 μM indole treatments (Figure S7b). Previous work suggested that indole-to-IAA conversion can be achieved through two synthesis routes: an indirect, tryptophan-dependent pathway or a direct, tryptophan-independent pathway (Normanly *et al.*, 1993). We observed a great [^{13}C]tryptophan enrichment in [^{13}C]indole-treated seedlings (Figure S7b), therefore suggesting that indole can be slowly turned into IAA via the tryptophan-dependent pathway. Remarkably, the abundance in native free IAA did not significantly change in these treatments, indicating that the contribution of the indole-derived IAA to the plant's total IAA does not drastically perturbs IAA homeostasis in the whole seedling. However, one cannot exclude that subtle, highly-localized changes in free auxin originating from indole-to-IAA conversion may account for the auxin-like activities observed in some of our experiments.

Indole interferes with the TIR1 auxin-signalling machinery

Transfer of control-germinated seedlings to IAA-containing medium results in primary root growth inhibition caused by the excess of auxin. This inhibition was gradually released by increasing concentrations of indole, but not of tryptophan, in the IAA-supplemented medium (Figures 5c and S8). This suggested that beyond a certain concentration indole itself may act as or be processed to a signal that competes with auxin in signalling independently from tryptophan-dependent IAA synthesis or IAA transport. Therefore, we next used seedlings expressing the AUX/IAA28 domain II-based auxin sensor DII-VENUS (Brunoud *et al.*, 2012) to investigate if indole would specifically compete with auxin signalling through the SCF^{TIR1} ubiquitin-ligase auxin receptor complex (Tan *et al.*, 2007). As previously published (Brunoud *et al.*, 2012), treatment with 50 nM IAA resulted in a rapid degradation of the nuclear DII-VENUS fluorescent signal (Figure 5d,e). However, in the presence of both indole and IAA the signal was indistinguishable from controls after 16 h of exposure while indole alone had minor effects, precluding that indole is a general proteasome inhibitor. Consistently, seedlings continuously grown on low amounts of indole retained the nuclear DII-VENUS fluorescent signal in a concentration-dependent manner but did not show altered expression of the auxin non-responsive mDII-VENUS reporter (Brunoud *et al.*, 2012) (Figure 5f). In order to verify the specificity of the indole signal on AUX/IAA peptides degradation we assessed indole-auxin competition using HS:AXR3/IAA17-GUS reporter lines (Gray *et al.*, 2001; Figure S9). After heat-shock, the AXR3-GUS signal consistently decreased in NAA treatments while indole-NAA co-application retained GUS activity. Thus, partial indole conversion into IAA does not fully explain the observed physiological and molecular effects in indole-treated seedlings. We therefore hypothesize that bacterial indole can act as a bimodal, tissue-dependent signal that triggers auxin-like responses at low concentrations and represses the auxin-signalling pathway upstream of the ubiquitin-mediated degradation of AUX/IAA proteins at higher concentrations.

DISCUSSION

Bacterial volatile organic compounds stimulate the secondary root system through auxin signalling

Early reports of VOCs-mediated growth promotion in *Arabidopsis* suggested that the phytohormone auxin plays a central role in this plant–microbe communication process (Ryu *et al.*, 2003; Zhang *et al.*, 2007). Microarray experiments revealed that *Bacillus subtilis* strain GB03 volatiles, devoid of known plant hormones, regulated auxin homeostasis and cell expansion in a tissue-dependent manner in plants after exposure (Zhang *et al.*, 2007). However, this pioneering work focused on the aerial parts of the plant and the effect of VOCs on the root system has not been investigated, although several reasons suggest that roots, rather than shoots, might be the target of choice for bacte-

http://doc.rero.ch

rial volatile-mediated plant growth manipulation: (i) the rhizosphere is a microbe-rich, dynamic environment and a known hotspot for inter-species communication; (ii) the root represents the most probable interface for volatile underground signals that can accumulate in soil pores; and (iii) the post-embryonic root development is an auxin-driven plastic process that rapidly adapts to external changes.

Recent studies have tackled this challenge. In 2007, López-Bucio *et al.* co-cultivated *Arabidopsis* seedlings with *Bacillus megaterium* and described a clear inhibition of primary root length accompanied with a promotion of secondary root and root hair formation. However, these effects could not be ascribed solely to volatile signals. Zamioudis *et al.* (2013) reported similar results after exposing *Arabidopsis* to *Pseudomonas* spp. strains and suggested that VOCs were a determinant signal to stimulate LR formation. The post-embryonic LR organogenesis process is under the control of PAT (Casimiro *et al.*, 2001; Bhalerao *et al.*, 2002) and several successive auxin signalling modules that rely on the stability of discrete AUX/IAA transcriptional regulators (De Rybel *et al.*, 2010; Goh *et al.*, 2012; Lavenus *et al.*, 2013). Plants impaired in canonical auxin-signalling components (AXR1/RUB1, AXR2/IAA7, AXR4/RGR1, ARF7 and ARF19) or auxin transporters (AUX1, PIN2, 3 and 7, ABCB1 and 19) were indistinguishable from the wild-type in their response to the bacterial stimuli (López-Bucio *et al.*, 2007; Zamioudis *et al.*, 2013; Figure S10). However, the auxin perception triple mutant *tir1afb2afb3,* which is defective for auxin F-box receptors, lost the ability to respond to LR-promoting *P. fluorescens* signals (Zamioudis *et al.*, 2013). Taken together, these data suggest that the positive effects of bacterial VOCs on lateral root formation do not interfere with PAT and directly involve auxin receptors. Therefore, active candidate molecules from the bacterial VOCs bouquet should fulfil these criteria. No such volatile effector has been characterised so far, though our work has identified indole as a potent VOC in plant-growth promotion (Blom *et al.*, 2011).

Indole interferes with auxin perception and stimulates lateral root formation

Here we show that indole stimulates LR formation by triggering the appearance of LRP along the growing root axis, but showing no drastic disturbances in root development or patterning. The bacterial indole-induced signal enters into and circulates within plant tissues independently of PAT and without significantly impacting auxin transport. However, this signal requires a functional PAT machinery to perform, suggesting that indole or indole-derived metabolites may directly act on auxin signalling to ultimately trigger the formation of LRPs. Indole itself is unlikely to exhibit auxin activity (Thimann, 1958) but is suspected to be a precursor in the biosynthesis of IAA (Ouyang *et al.*, 2000; Liu *et al.*, 2011). Indeed treated seedlings can partially convert indole into IAA, most likely via tryptophan-dependant synthesis in high auxin producing meristematic regions. Although a slow conversion of indole into auxin and subsequent auxin accumulation would explain a part of the classic auxin-related responses reported here, several results are inconsistent with this simple explanation. First, indole competes with IAA and synthetic auxins for primary root elongation inhibition, while tryptophan treatments do not, suggesting that part of the indole effects reported here are independent from auxin biosynthesis. Second, although IAA issued from exogenous indole could potentially trigger the priming of LR founder cells, NPA treatments upstream the indole source prevented LR appearance, inferring that local indole-to-IAA conversion may not be sufficient to achieve this task. Third, in saturating IAA treatments where indole-to-IAA conversion is not expected to play a critical role, seedlings responded to indole treatments in forming more LRs that failed to fully elongate. Similar treatments with synthetic auxins resulted in different LR behaviour, such as an indole-mediated partial release of 2,4-D-induced developmental defects (Figure S4c) that could not be obtained with extra IAA. The same line of reasoning applies to the strong indole-induced adventitious roots promotion or apical hook maintenance, a response opposite to the reported hookless hypocotyls induced by exogenous auxins or ATIs treatments and observed in auxin-overproducing *Arabidopsis* mutants such as *sur1*/*alf1*/*hls3* (Boerjan *et al.*, 1995; Celenza *et al.*, 1995; Lehman *et al.*, 1996). Finally, these counterintuitive indole effects on plant physiology cannot be directly imputed to strong alterations of auxin homeostasis since high indole treatments did not reveal dramatic changes in natural free IAA contents either in seedlings roots or shoots, as reported earlier for 4,4,4-trifluoro-3-(indole-3-)butyric acid and PCIB (Zhao and Hasenstein, 2010).

Therefore, beyond its conversion into IAA that could account for the observed auxin-like responses, it is tempting to postulate that indole itself or an indole derivative can participate in auxin-controlled developmental events such as LR formation. The *alf3-1* mutant, impaired in the uncharacterised ABERRANT LATERAL ROOT FORMATION3 gene (ALF3, Celenza *et al.*, 1995), forms twice as many LRPs that fail to emerge compared with wt plants, a phenotype which could be rescued by continuous supply of indole, but not of tryptophan. Nevertheless, transfer of *alf3-1* seedlings grown on indole-free medium to 80 μM indole did not rescue the pre-existing arrested LRPs but rather triggered growth of new LRs (Celenza *et al.*, 1995). One interpretation could be that an indole signal is required throughout LR development or that an indole-IAA synergism participates in root formation as suggested in pioneer studies (Van Raalte, 1951; Gorter, 1958).

Given the fact that indole competes with IAA and synthetic auxins for primary root elongation and AUX/IAA-

http://doc.rero.ch

based auxin signalling, the accumulation of an indole-derived IAA antagonist with properties similar to putative anti-auxins could be an alternative hypothesis. Changes in AUX/IAA stability induced by *p*-chlorophenoxyisobutyric acid (Oono *et al.*, 2003), toyocamycin (Hayashi *et al.*, 2009), terfestatin A (Yamazoe *et al.*, 2005), yokonolide B (Hayashi *et al.*, 2003) and α-alkyl IAA derivative (Hayashi *et al.*, 2008) treatments altered auxin-induced LR formation while yokonolide B alone promoted LR appearance at low concentrations, inferring that these molecules modulate auxin signalling in a similar manner as indole.

Therefore, we hypothesize that an indole-derived signal could compete for auxin at the TIR1/AFB level by preventing the degradation of AUX/IAA peptides. Auxin perception is thought to be achieved by co-receptor complexes formed by a combination of TIR1/AFB and AUX/IAA proteins that provide ligand selectivity and thus sustain a dynamic range of responses to the hormone (Havens *et al.*, 2012; Villalobos *et al.*, 2012; Lavenus *et al.*, 2013). Given the diversity of TIR1/AFB and AUX/IAA proteins (reviewed in Finet *et al.*, 2013 and Reed, 2001), an indole-derived signal could therefore redirect the root post-embryonic development program by modulating the auxin signal transduction cascade.

Is the AUX/IAA peptide turnover the key to volatile-mediated plant-bacteria interactions?

There is increasing evidence that interactions between auxin and classical phytohormones signalling pathways, such as salicylic acid, abscisic acid, cytokinins and brassinosteroids, play a substantial role in plant-microbe interactions (Spoel and Dong, 2008; Grant and Jones, 2009; Kazan and Manners, 2009; Robert-Seilaniantz *et al.*, 2011). Unfortunately, most of the effort to characterize these interactions at the molecular level has focused on pathogenic rather than mutualistic interactions. Plants infected with phytopathogenic bacteria such as *Xanthomonas* spp. or *P. syringae* have been reported to display increased levels of free auxin and exogenous auxin has been shown to stimulate disease susceptibility (O'Donnell *et al.*, 2003; Chen *et al.*, 2007; Wang *et al.*, 2007). The perturbation of hormonal perception or homeostasis seems to represent a general virulence strategy for pathogenic microorganisms, thus, the SCF^{TIR1} auxin receptor complex represents a target of choice for rapid and effective manipulations of plant responses at the crossroads of defence and growth programs. Apart from well known plant pathogens, which either produce auxin or manipulate plant auxin biosynthesis (Spaepen *et al.*, 2007), other microbial strategies to manipulate auxin perception have been reported. The *P. syringae* type III effector AvrRpt2 has been shown to act with auxin to stimulate AUX/IAA proteins turnover, probably at the level of the degradosome (Chen *et al.*, 2007; Cui *et al.*, 2013). Furthermore, recent work showed that microbial associated molecular patterns (MAMPs; reviewed in (Boller and Felix, 2009)) down-regulate auxin signalling in *Arabidopsis* by targeting TIR1, AFB2, and AFB3 auxin receptor transcript levels through miRNA silencing (Navarro *et al.*, 2006). Finally, salicylic acid treatment strongly represses auxin-related genes expression and impedes auxin response by stabilizing AUX/IAA proteins (Wang *et al.*, 2007). Hence, the stability of the auxin perception mechanism is of pivotal importance for plant-microbe interactions and the suppression of auxin signalling could be part of a plant defence strategy.

The signalling events triggered by MAMPs lead to two typical plant responses, ethylene production (Boller, 1982) and oxidative burst (Lamb and Dixon, 1997), that are not activated by indole treatments (Blom *et al.*, 2011). Nonetheless, indole blocked the flagellin-based elicitation of ethylene production and increased and sustained oxidative burst in the same conditions (Blom *et al.*, 2011). This argues for the indole signal not to be recognized as a MAMP and to presumably circumvent the defence response. Although it cannot be excluded that plants recognize indole as a microbial volatile-associated molecular pattern (mVAMP) and engage WRKY-type transcription factors, as recently proposed by (Wenke *et al.*, 2012), no direct evidence is available that supports a role for indole in volatile-mediated pathogen-responsive signalling. Contrary to the deleterious effects of *Serratia plymuthica* or *Stenotrophomonas maltophilia* VOCs on *Arabidopsis* reported by Wenke *et al.* (2012), indole acts as a positive signal for root-system development and growth.

A bimodal mode of action of the indole signal through the production of auxin and of an indole derivative holding *in planta* anti-auxin activity that participates in lateral root formation would represent a non-invasive microbial strategy to bypass the deleterious effects of exogenous auxin on root growth and disease resistance. The repressing activity could ensure a continuum in the indole-induced changes triggered in the plant architecture initiated at low concentrations in presumably very localised area. As a result, the secondary root system expands without affecting primary root development, which likely may enrich the rhizosphere for root exudates that microorganisms use as a food source. Hence, remote manipulation of the plant hormonal system could be an effective mechanism by which bacteria directly modify their ecological niche to their advantage. Knowledge of inter-kingdom volatile communications in soil may prove useful for designing cost-effective sustainable agricultural strategies.

EXPERIMENTAL PROCEDURES

Arabidopsis thaliana lines, bacterial strains and chemicals

All experiments were performed with the *A. thaliana* Columbia-0 ecotype. DII-VENUS (Brunoud *et al.*, 2012) (N799173, N799174) and

http://doc.rero.ch

HS::AXR3NT-GUS (Gray *et al.*, 2001) (N9570, N9571, N9572) lines were obtained from the Nottingham Arabidopsis Stock Centre (UK). *DR5::GUS* and *DR5::GFP* lines (Ulmasov *et al.*, 1997; Ottenschlager *et al.*, 2003) were kindly provided by Prof. Enrico Martinoia and Dr. Markus Geisler, respectively. All experiments were performed with bacterial strains described earlier (Blom *et al.*, 2011). The *E. coli tnaA* deletion mutant (JW3686) was obtained from the Keio stock collection (Keio, Japan). Indole, 3-indoleacetic acid, L-tryptophan, 1-*N*-naphtylphtalamic acid, 2-napthoxyacetic acid, 2,4-dichlorophenoxyacetic acid, 5-bromo-4-chloro-3-indolyl β-D-glucuronide and 4-methylumbelliferyl-β-D-glucuronide were obtained from Sigma-Aldrich; http://www.sigmaaldrich.com). [2-^{14}C]-indole was obtained from American Radiolabeled Chemicals (http://www.arc-inc.com/). [5-^{3}H]- and [^{2}H]-indoleacetic acid were kindly provided by Dr. Markus Geisler. [PHENYL-^{13}C6]- and [2-^{13}C]-indole were obtained from Cambridge Isotope Laboratories; (http://www.isotope.com/) .

Culture conditions

Unless otherwise indicated, seedlings were surface-sterilised and grown on Parafilm®-sealed vertical plates containing 0.5 × Murashige and Skoog (MS) medium (Sigma-Aldrich), 1% sucrose, 1.5% agar, pH to 5.7 with KOH, in the dark or at 12 h 100 μE light per day at 20°C. Images were acquired using either a CanonScan 8600F flatbed scanner (Canon Inc.; http://www.canon.com/) or a M165FC microscope (Leica; http://www.leica-microsystems.com/) and growth and secondary root parameters were quantified using NIH IMAGEJ. Bacterial strains were cultured in Luria-Bertani broth (Difco; http://www.bdbiosciences.com) and/or MS medium under plant-growth conditions or at 37°C. In total, 20 μl of a liquid bacterial culture of OD_{600} 0.8 was inoculated, simultaneously to seedling sowing, on 1.5% agar Luria-Bertani in the middle of the stainless steel ring delimiting the bacterial compartment.

Endogenous and indole-derived IAA and tryptophan analysis

For endogenous free auxin quantification, shoot and root segments of 120 seedlings per sample were collected and pooled 24 h after 10 μM indole treatments. The samples were subsequently handled as in (Bouchard *et al.*, 2006). Determination of [2-^{13}C]-indole conversion was performed as follow: shoot and root segments of 120 seedlings per sample were collected and pooled 24 h after indicated [2-^{13}C]-indole treatments, extracted in MetOH: isopropanol:glacial acetic acid (20:79:1) and supernatant fractions were evaporated. For derivatisation of IAA, each sample was dissolved in 700 μl (dichloromethane/isopropanol 4:1) and 4 μl 2.0 M trimethylsilyldiazomethane in hexane was added. The vial was vial capped and allowed to sit at room temperature for 30 min. Then 4 μl 2.0 M acetic acid in hexane was added and the solvent was removed (Schmelz *et al.*, 2003). The sample was diluted with 100 μl dichloromethane and 1 μl was injected into the GC/MS system. For the analysis of the tryptophan, the dichloromethane was evaporated and the residue dissolved in 100 μl water/ethanol/pyridine in a ratio of 60:32:8. Then 5 μl methyl chloroformiate (mcf) was added, the vial was capped and shaken for 5 sec. Afterwards 100 μl dichloromethane containing 1% mcf was added, the organic phase separated and dried with NaCl. Finally, 1 μl was injected into the GC/MS system (Husek, 1991).

Headspace volatile analysis

Bacterial volatiles emitted by agar plate cultures were collected using a closed-loop stripping apparatus (CLSA). In this system, air was continuously pumped (MB-21E, Senior Flextronics; http://www.senior-flexonics.com) through a closed system over the agar plate and directed through a charcoal filter (Chromtech GmbH; http://www.chromtech.de Idstein, Precision Charcoal Filter, 5 mg) for 24 h. The charcoal filter was extracted three times with 10–15 μl analytically pure dichloromethane (≥99.8%, Merck; http://www.merck.com). Extracts were analysed by gas chromatography coupled with a mass selective detector (GC-MS, GC 7890A/MSD 5975C, Agilent Technologies; http://www.agilent.com). The GC-MS system was equipped with a HP-5 ms fused silica capillary column (30 m, 0.22 mm internal diameter, 0.25 μm film, Agilent Technologies). Conditions were as follows: inlet pressure: 67 kPa, He-flow: 24.2 ml/min, injector: 250°C, transfer line 300°C, electron energy 70 eV. The GC oven temperature was kept at 50°C for 5 min, followed by raising the temperature with 5°C/min to 320°C. The identification of compounds was performed by comparison of their mass spectra and retention indices (determined from a homologous series on n-alkanes (C8-C32)) with those of reference compounds and commercial mass spectral libraries (Wiley 7, NIST 08).

Arabidopsis thaliana physiological assays

Root gravitropism was determined as follows: 5-day-old vertically grown seedlings were transferred, vertically aligned onto fresh plates supplemented with the required treatments and let grow for another 16 h. Two consecutive gravistimulations were then applied by rotating the plates 90°. Primary root tip orientation relative to the gravity vector was determined using NIH IMAGEJ (http://rsb.info.nih.gov/ij/). For skotomorphogenetic assays, seedlings were grown for 5 days in the dark, then hypocotyl length, relative angle to the gravity vector and the relative angle formed at the hypocotyl apical hook were measured using NIH IMAGEJ. Adventitious root formation was triggered by photostimulating 5-day-old etiolated seedlings for 1 h and letting the plants either grow in standard light or dark conditions for another 5 days. Adventitious roots were then counted under a M165FC microscope (Leica, Germany).

β-Glucuronidase activity assays and histochemical staining

DR5::GUS seedlings were grown for the specified amount of time with indicated treatments. A 5-mm segment from the root tip was excised from the rest of the root and 30 plants were pooled per sample extraction in 150 mM sodium phosphate pH 7.0, 10 mM EDTA, 10 mM β-mercaptoethanol, 0.1% Triton X-100, 0.1% sarcosyl, 140 μM PMSF. Fluorometric quantitative measurements of GUS activity were obtained after 30 min incubation at 37°C using 4-methylumbelliferyl β-D-glucuronide as substrate and standardized to sample protein concentration. Histochemical stainings were carried out overnight at room temperature in 150 mM sodium phosphate pH 7.0, 0.5 mM $K_3Fe(CN)_6$ and 0.1% Triton X-100 using 5-bromo-4-chloro-3-indolyl β-D-glucuronide as substrate and tissues were cleared in 70% ethanol.

Microscopy and image analysis

Primary root tip *DR5::GUS* histochemical stainings were imaged using a Leica M165FC microscope. *DR5::GFP* fluorescent signals were acquired using a Leica DM6000 B microscope or a Leica DM5500Q confocal LASER scanning microscope (Leica, Germany) and pixel intensities were analysed using NIH IMAGEJ. DII-VENUS and mDII-VENUS fluorescent signals were acquired using a Leica DM5500Q confocal LASER scanning microscope. Maximum projections of 40 1.5-μm slices per sample were generated using the Leica LAS AF software and nuclear fluorescence was quantified using NIH IMAGEJ with an intensity threshold of 25 per pixel.

http://doc.rero.ch

Radiolabelled transport and imaging

Radiolabelled indole and IAA transport assays were essentially carried out as described (Lewis and Muday, 2009). Agarose beads containing [^{14}C]-indole and solvent, NPA or NOA were placed over the primary root tip (basipetal) or the root–shoot junction (acropetal) of 5-day-old seedlings transferred to fresh growth medium. After incubation 5-mm segments were excised 3 mm from the radioactive source, 10 plants were pooled per sample, homogenized in 3 ml Ultima Gold scintillation liquid (Perkin-Elmer; http://www.perkinelmer.com) and the amount of radioactivity measured in a Tri-Carb 2900TR liquid scintillation analyser (Packard; http://www.perkinelmer.com). For indole homologous competition transport assays agarose beads containing [^{14}C]-indole and solvent or increasing concentrations of cold indole were placed over the primary root tip of 5-day-old seedlings transferred to fresh growth medium. After 16 h of transport the apical 3 mm of the root was excised and discarded and the amount of radioactivity in each subsequent 5-mm segment from the root tip was measured. Sample autoradiograms were obtained using a Cyclone Super Resolution storage phosphor screen system (Packard).

Data analysis

Data were analysed using the GraphPad Quikcalcs tools (http://www.graphpad.com/quickcalcs/), GRAPHPAD PRISM 5 software and Microsoft Excel software.

ACKNOWLEDGMENTS

We are grateful to Prof. E. Martinoia for continuous support and for providing the *DR5::GUS Arabidopsis* lines. We are thankful to L. Charrier, P. Düchting, R. Baumgartner, L. Hunziker and A. Gardiner for technical assistance and Dr. K. Agnoli for proofreading. A.B. thanks F. Meins, J. Friml and T. Boller for comments and suggestions. This work was funded through a Plant Science Centre-Syngenta Fellowship and to A.B. and partially financed by the Swiss National Science Foundation (grant 31003A-149271 to L.W.).

SUPPORTING INFORMATION

Additional Supporting Information may be found in the online version of this article.

Figure S1. Bacterial VOCs remotely affect root growth and development.

Figure S2. Effects of indole on the primary root tip extension of excised seedlings.

Figure S3. Volatile indole moves *in planta* and accumulates in sites of auxin action.

Figure S4. Indole alters responses to synthetic auxins

Figure S5. Indole treatment increases *DR5::GFP* signal intensity in the root tip and at the root-shoot junction but does not alter tissue distribution.

Figure S6. Continuous indole treatments trigger apical DR5::GUS signal patterns similar to *E. coli* wt VOCs in primary root tips.

Figure S7. Indole can slowly be converted to tryptophan and free IAA.

Figure S8. Indole but not tryptophan releases the primary root tip growth inhibition induced by 50 nM IAA.

Figure S9. Indole-auxin co-application prevents auxin-induced AXR3/IAA17 degradation.

Figure S10. The auxin transport mutants *abcb19* and *abcb1x19* respond similarly to *E. coli* VOCs and indole treatments.

Table S1 List of volatile organic compounds emitted by *E. coli* JM105 and corresponding *tnaA* mutant grown on solid agar Luria-Bertani medium.

REFERENCES

Anyanful, A., Dolan-Livengood, J.M., Lewis, T., Sheth, S., DeZalia, M.N., Sherman, M.A., Kalman, L.V., Benian, G.M. and Kalman, D. (2005) Paralysis and killing of *Caenorhabditis elegans* by enteropathogenic *Escherichia coli* requires the bacterial tryptophanase gene. *Mol. Microbiol.*, **57**, 988–1007.

Bais, H.P., Park, S.W., Weir, T.L., Callaway, R.M. and Vivanco, J.M. (2004) How plants communicate using the underground information superhighway. *Trends Plant Sci.*, **9**, 26–32.

Bansal, T., Alaniz, R.C., Wood, T.K. and Jayaraman, A. (2010) The bacterial signal indole increases epithelial-cell tight-junction resistance and attenuates indicators of inflammation. *Proc. Natl Acad. Sci. USA*, **107**, 228–233.

Bhalerao, R.P., Eklof, J., Ljung, K., Marchant, A., Bennett, M. and Sandberg, G. (2002) Shoot-derived auxin is essential for early lateral root emergence in *Arabidopsis* seedlings. *Plant J.* **29**, 325–332.

Bhattacharyya, P.N. and Jha, D.K. (2012) Plant growth-promoting rhizobacteria (PGPR): emergence in agriculture. *World J. Microbiol. Biotechnol.*, **28**, 1327–1350.

Blom, D., Fabbri, C., Connor, E.C., Schiestl, F.P., Klauser, D.R., Boller, T., Eberl, L. and Weisskopf, L. (2011) Production of plant growth modulating volatiles is widespread among rhizosphere bacteria and strongly depends on culture conditions. *Environ. Microbiol.*, **13**, 3047–3058.

Boerjan, W., Cervera, M.T., Delarue, M., Beeckman, T., Dewitte, W., Bellini, C., Caboche, M., Vanonckelen, H., Vanmontagu, M. and Inze, D. (1995) Superroot, a recessive mutation in *Arabidopsis*, confers auxin overproduction. *Plant Cell*, **7**, 1405–1419.

Boller, T. (1982) Ethylene-induced biochemical defenses against pathogens. In *Plant Growth Substances*. (Wareing, P.F., ed). New York: Academic Press, pp. 303–312.

Boller, T. and Felix, G. (2009) A renaissance of elicitors: perception of microbe-associated molecular patterns and danger signals by pattern-recognition receptors. *Annu. Rev. Plant Biol.*, **60**, 379–406.

Bouchard, R., Bailly, A., Blakeslee, J.J. *et al.* (2006) Immunophilin-like TWISTED DWARF1 modulates auxin efflux activities of *Arabidopsis* P-glycoproteins. *J. Biol. Chem.*, **281**, 30603–30612.

Brunoud, G., Wells, D.M., Oliva, M. *et al.* (2012) A novel sensor to map auxin response and distribution at high spatio-temporal resolution. *Nature*, **482**, 103–106.

Bulgarelli, D., Rott, M., Schlaeppi, K. *et al.* (2012) Revealing structure and assembly cues for *Arabidopsis* root-inhabiting bacterial microbiota. *Nature*, **488**, 91–95.

Casimiro, I., Marchant, A., Bhalerao, R.P. *et al.* (2001) Auxin transport promotes *Arabidopsis* lateral root initiation. *Plant Cell*, **13**, 843–852.

Celenza, J.L., Grisafi, P.L. and Fink, G.R. (1995) A pathway for lateral root-formation in *Arabidopsis thaliana*. *Genes Dev.*, **9**, 2131–2142.

Chant, E.L. and Summers, D.K. (2007) Indole signalling contributes to the stable maintenance of *Escherichia coli* multicopy plasmids. *Mol. Microbiol.*, **63**, 35–43.

Chen, Z.Y., Agnew, J.L., Cohen, J.D., He, P., Shan, L.B., Sheen, J. and Kunkel, B.N. (2007) *Pseudomonas syringae* type III effector AvrRpt2 alters *Arabidopsis thaliana* auxin physiology. *Proc. Natl Acad. Sci. USA*, **104**, 20131–20136.

Chimerel, C., Murray, A.J., Oldewurtel, E.R., Summers, D.K. and Keyser, U.F. (2013) The effect of bacterial signal indole on the electrical properties of lipid membranes. *ChemPhysChem*, **14**, 417–423.

Contreras-Cornejo, H.A., Macias-Rodriguez, L., Cortes-Penagos, C. and Lopez-Bucio, J. (2009) *Trichoderma virens*, a plant beneficial fungus, enhances biomass production and promotes lateral root growth through an auxin-dependent mechanism in *Arabidopsis*. *Plant Physiol.*, **149**, 1579–1592.

Cui, F., Wu, S., Sun, W., Coaker, G., Kunkel, B., He, P. and Shan, L. (2013) The *Pseudomonas syringae* type III effector AvrRpt2 promotes pathogen virulence via stimulating *Arabidopsis* auxin/indole acetic acid protein turnover. *Plant Physiol.*, **162**, 1018–1029.

http://doc.rero.ch

http://doc.rero.ch

De Rybel, B., Vassileva, V., Parizot, B. *et al.* (2010) A novel Aux/IAA28 signaling cascade activates GATA23-dependent specification of lateral root founder cell identity. *Curr. Biol.*, **20**, 1697–1706.

De Smet, I., Tetsumura, T., De Rybel, B. *et al.* (2007) Auxin-dependent regulation of lateral root positioning in the basal meristem of *Arabidopsis*. *Development*, **134**, 681–690.

Di Martino, P., Fursy, R., Bret, L., Sundararaju, B. and Phillips, R.S. (2003) Indole can act as an extracellular signal to regulate biofilm formation of *Escherichia coli* and other indole-producing bacteria. *Can. J. Microbiol.*, **49**, 443–449.

Dubrovsky, J.G., Sauer, M., Napsucialy-Mendivil, S., Ivanchenko, M.G., Friml, J., Shishkova, S., Celenza, J. and Benkova, E. (2008) Auxin acts as a local morphogenetic trigger to specify lateral root founder cells. *Proc. Natl Acad. Sci. USA*, **105**, 8790–8794.

Felten, J., Kohler, A., Morin, E., Bhalerao, R.P., Palme, K., Martin, F., Ditengou, F.A. and Legue, V. (2009) The ectomycorrhizal fungus *Laccaria bicolor* stimulates lateral root formation in poplar and *Arabidopsis* through auxin transport and signaling. *Plant Physiol.*, **151**, 1991–2005.

Finet, C., Berne-Dedieu, A., Scutt, C.P. and Marletaz, F. (2013) Evolution of the ARF gene family in land plants: old domains, new tricks. *Mol. Biol. Evol.*, **30**, 45–56.

Goh, T., Kasahara, H., Mimura, T., Kamiya, Y. and Fukaki, H. (2012) Multiple AUX/IAA-ARF modules regulate lateral root formation: the role of *Arabidopsis* SHY2/IAA3-mediated auxin signalling. *Philos. Trans. R. Soc. Lond., B, Biol. Sci.* **367**, 1461–1468.

Gorter, C.J. (1958) Synergism of indole and indole-3-acetic acid in the root production of *Phaseolus* cuttings. *Physiol. Plant.*, **11**, 1–9.

Grant, M.R. and Jones, J.D.G. (2009) Hormone (dis)harmony moulds plant health and disease. *Science*, **324**, 750–752.

Gray, W.M., Kepinski, S., Rouse, D., Leyser, O. and Estelle, M. (2001) Auxin regulates SCF(TIR1)-dependent degradation of AUX/IAA proteins. *Nature*, **414**, 271–276.

Han, Y., Yang, C.L., Yang, Q., Qi, Z.Z., Liu, W.Z., Xu, Z.H., Zhu, W.M., Bossier, P. and Zhang, X.H. (2011) Mutation of tryptophanase gene tnaA in *Edwardsiella tarda* reduces lipopolysaccharide production, antibiotic resistance and virulence. *Environ. Microbiol. Rep.* **3**, 603–612.

Havens, K.A., Guseman, J.M., Jang, S.S., Pierre-Jerome, E., Bolten, N., Klavins, E. and Nemhauser, J.L. (2012) A synthetic approach reveals extensive tunability of auxin signaling. *Plant Physiol.*, **160**, 135–142.

Hayashi, K., Jones, A.M., Ogino, K., Yamazoe, A., Oono, Y., Inoguchi, M., Kondo, H.Nozaki, H. (2003) Yokonolide B, a novel inhibitor of auxin action, blocks degradation of AUX/IAA factors. *J. Biol. Chem.*, **278**, 23797–23806.

Hayashi, K., Tan, X., Zheng, N., Hatate, T., Kimura, Y., Kepinski, S. and Nozaki, H. (2008) Small-molecule agonists and antagonists of F-box protein-substrate interactions in auxin perception and signaling. *Proc. Natl Acad. Sci. USA*, **105**, 5632–5637.

Hayashi, K., Karnio, S., Oono, Y., Townsend, L.B. and Nozaki, H. (2009) Toyocamycin specifically inhibits auxin signaling mediated by SCFTIR1 pathway. *Phytochemistry*, **70**, 190–197.

Husek, P. (1991) Rapid derivatization and gas-chromatographic determination of amino-acids. *J. Chromatogr.*, **552**, 289–299.

Kai, M. and Piechulla, B. (2009) Plant growth promotion due to rhizobacterial volatiles - An effect of CO_2? *FEBS Lett.*, **583**, 3473–3477.

Kazan, K. and Manners, J.M. (2009) Linking development to defense: auxin in plant-pathogen interactions. *Trends Plant Sci.*, **14**, 373–382.

Kwon, Y.S., Ryu, C.M., Lee, S. *et al.* (2010) Proteome analysis of *Arabidopsis* seedlings exposed to bacterial volatiles. *Planta*, **232**, 1355–1370.

Lamb, C. and Dixon, R.A. (1997) The oxidative burst in plant disease resistance. *Annu. Rev. Plant Physiol. Plant Mol. Biol.* **48**, 251–275.

Lavenus, J., Goh, T., Roberts, I., Guyomarc'h, S., Lucas, M., De Smet, I., Fukaki, H., Beeckman, T., Bennett, M. and Laplaze, L. (2013) Lateral root development in *Arabidopsis*: fifty shades of auxin. *Trends Plant Sci.*, **18** (8), 450–458.

Lee, J.T., Jayaraman, A. and Wood, T.K. (2007) Indole is an inter-species biofilm signal mediated by SdiA. *BMC Microbiol.*, **7**, 42.

Lee, H.H., Molla, M.N., Cantor, C.R. and Collins, J.J. (2010) Bacterial charity work leads to population-wide resistance. *Nature*, **467**, 82–85.

Lee, J.-H., Cho, H., Kim, Y., Kim, J.-A., Banskota, S., Cho, M. and Lee, J. (2013) Indole and 7-benzyloxyindole attenuate the virulence of *Staphylococcus aureus*. *Appl. Microbiol. Biotechnol.*, **97**, 4543–4552.

Lehman, A., Black, R. and Ecker, J.R. (1996) HOOKLESS1, an ethylene response gene, is required for differential cell elongation in the *Arabidopsis* hypocotyl. *Cell*, **85**, 183–194.

Lewis, D.R. and Muday, G.K. (2009) Measurement of auxin transport in *Arabidopsis thaliana*. *Nat. Protoc.*, **4**, 437–451.

Liu, X., Cohen, J.D. and Gardner, G. (2011) Low-fluence red light increases the transport and biosynthesis of auxin. *Plant Physiol.*, **157**, 891–904.

López-Bucio, J., Campos-Cuevas, J.C., Hernández-Calderón, E., Velásquez-Becerra, C., Farias-Rodríguez, R., Macías-Rodríguez, L.I. and Valencia-Cantero, E. (2007) *Bacillus megaterium* rhizobacteria promote growth and alter root-system architecture through an auxin- and ethylene-independent signaling mechanism in *Arabidopsis thaliana*. *Mol. Plant Microbe Interact.*, **20**, 207–217.

Lundberg, D.S., Lebeis, S.L., Paredes, S.H. *et al.* (2012) Defining the core *Arabidopsis thaliana* root microbiome. *Nature*, **488**, 86–90.

Meldau, D.G., Meldau, S., Hoang, L.H., Underberg, S., Wunsche, H. and Baldwin, I.T. (2013) Dimethyl disulfide produced by the naturally associated bacterium *Bacillus* sp. B55 promotes *Nicotiana attenuata* growth by enhancing sulfur nutrition. *Plant Cell*, **25**, 2731–2747.

Navarro, L., Dunoyer, P., Jay, F., Arnold, B., Dharmasiri, N., Estelle, M., Voinnet, O. and Jones, J.D.G. (2006) A plant miRNA contributes to antibacterial resistance by repressing auxin signaling. *Science*, **312**, 436–439.

Normanly, J., Cohen, J.D. and Fink, G.R. (1993) *Arabidopsis thaliana* auxotrophs reveal a tryptophan-independent biosynthetic pathway for indole-3-acetic acid. *Proc. Natl Acad. Sci. USA*, **90**, 10355–10359.

O'Donnell, P.J., Schmelz, E.A., Moussatche, P., Lund, S.T., Jones, J.B. and Klee, H.J. (2003) Susceptible to intolerance - a range of hormonal actions in a susceptible *Arabidopsis* pathogen response. *Plant J.* **33**, 245–257.

Oono, Y., Ooura, C., Rahman, A., Aspuria, E.T., Hayashi, K., Tanaka, A. and Uchimiya, H. (2003) *p*-Chlorophenoxyisobutyric acid impairs auxin response in *Arabidopsis* root. *Plant Physiol.*, **133**, 1135–1147.

Ortiz-Castro, R., Contreras-Cornejo, H.A., Macias-Rodriguez, L. and Lopez-Bucio, J. (2009) The role of microbial signals in plant growth and development. *Plant Signal. Behav.*, **4**, 701–712.

Ottenschlager, I., Wolff, P., Wolverton, C., Bhalerao, R.P., Sandberg, G., Ishikawa, H., Evans, M. and Palme, K. (2003) Gravity-regulated differential auxin transport from columella to lateral root cap cells. *Proc. Natl Acad. Sci. USA*, **100**, 2987–2991.

Ouyang, J., Shao, X. and Li, J. (2000) Indole-3-glycerol phosphate, a branchpoint of indole-3-acetic acid biosynthesis from the tryptophan biosynthetic pathway in *Arabidopsis thaliana*. *Plant J.* **24**, 327–333.

Reed, J.W. (2001) Roles and activities of Aux/IAA proteins in *Arabidopsis*. *Trends Plant Sci.*, **6**, 420–425.

Reed, R.C., Brady, S.R. and Muday, G.K. (1998) Inhibition of auxin movement from the shoot into the root inhibits lateral root development in Arabidopsis. *Plant Physiol.*, **118**, 1369–1378.

Robert-Seilaniantz, A., Grant, M. and Jones, J.D.G. (2011) Hormone crosstalk in plant disease and defense: more than just JASMONATE-SALICYLATE antagonism. *Annu. Rev. Phytopathol.*, **49**, 317–343.

Ryu, C.M., Farag, M.A., Hu, C.H., Reddy, M.S., Wei, H.X., Pare, P.W. and Kloepper, J.W. (2003) Bacterial volatiles promote growth in *Arabidopsis*. *Proc. Natl Acad. Sci. USA*, **100**, 4927–4932.

Schmelz, E.A., Engelberth, J., Alborn, H.T., O'Donnell, P., Sammons, M., Toshima, H. and Tumlinson, J.H. (2003) Simultaneous analysis of phytohormones, phytotoxins, and volatile organic compounds in plants. *Proc. Natl Acad. Sci. USA*, **100**, 10552–10557.

Schwark, A. and Schierle, J. (1992) Interaction of ethylene and auxin in the regulation of hook growth. 1. The role of auxin in different growing regions of the hypocotyl hook of *Phaseolus vulgaris*. *J. Plant Physiol.*, **140**, 562–570.

Spaepen, S., Vanderleyden, J. and Remans, R. (2007) Indole-3-acetic acid in microbial and microorganism-plant signaling. *FEMS Microbiol. Rev.*, **31**, 425–448.

Spoel, S.H. and Dong, X.N. (2008) Making sense of hormone crosstalk during plant immune responses. *Cell Host Microbe*, **3**, 348–351.

Tan, X., Calderon-Villalobos, L.I., Sharon, M., Zheng, C., Robinson, C.V., Estelle, M. and Zheng, N. (2007) Mechanism of auxin perception by the TIR1 ubiquitin ligase. *Nature*, **446**, 640–645.

Thimann, K.V. (1958) Auxin activity of some indole derivatives. *Plant Physiol.*, **33**, 311–321.

Ulmasov, T., Murfett, J., Hagen, G. and Guilfoyle, T.J. (1997) Aux/IAA proteins repress expression of reporter genes containing natural and highly active synthetic auxin response elements. *Plant Cell*, **9**, 1963–1971.

Van Raalte, M.H. (1951) Interaction between indole and hemi-auxins with indoleacetic acid in root formation. I and II. *Kon. Neder. Akad. Wetens. Proc.* **C54**, 117–125.

Vega, N.M., Allison, K.R., Khalil, A.S. and Collins, J.J. (2012) Signaling-mediated bacterial persister formation. *Nat. Chem. Biol.*, **8**, 431–433.

Vespermann, A., Kai, M. and Piechulla, B. (2007) Rhizobacterial volatiles affect the growth of fungi and *Arabidopsis thaliana*. *Appl. Environ. Microbiol.*, **73**, 5639–5641.

Villalobos, L.I.A.C., Lee, S., De Oliveira, C. *et al.* (2012) A combinatorial TIR1/AFB-Aux/IAA co-receptor system for differential sensing of auxin. *Nat. Chem. Biol.*, **8**, 477–485.

Wang, D., Ding, X. and Rather, P.N. (2001) Indole can act as an extracellular signal in *Escherichia coli*. *J. Bacteriol.*, **183**, 4210–4216.

Wang, D., Pajerowska-Mukhtar, K., Culler, A.H. and Dong, X.N. (2007) Salicylic acid inhibits pathogen growth in plants through repression of the auxin signaling pathway. *Curr. Biol.*, **17**, 1784–1790.

Wenke, K., Wanke, D., Kilian, J., Berendzen, K., Harter, K. and Piechulla, B. (2012) Volatiles of two growth-inhibiting rhizobacteria commonly engage AtWRKY18 function. *Plant J.* **70**, 445–459.

Wikoff, W.R., Anfora, A.T., Liu, J., Schultz, P.G., Lesley, S.A., Peters, E.C. and Siuzdak, G. (2009) Metabolomics analysis reveals large effects of gut microflora on mammalian blood metabolites. *Proc. Natl Acad. Sci.*, **106**, 3698–3703.

Yamamoto, M. and Yamamoto, K.T. (1998) Differential effects of 1-naphthaleneacetic acid, indole-3-acetic acid and 2,4-dichlorophenoxyacetic acid on the gravitropic response of roots in an auxin-resistant mutant of *Arabidopsis*, aux1. *Plant Cell Physiol.*, **39**, 660–664.

Yamazoe, A., Hayashi, K., Kepinski, S., Leyser, O. and Nozaki, H. (2005) Characterization of terfestatin A, a new specific inhibitor for auxin signaling. *Plant Physiol.*, **139**, 779–789.

Zamioudis, C., Mastranesti, P., Dhonukshe, P., Blilou, I. and Pieterse, C.M. (2013) Unraveling root developmental programs initiated by beneficial *Pseudomonas* spp. bacteria. *Plant Physiol.*, **162**, 304–318.

Zhang, H., Kim, M.S., Krishnamachari, V. *et al.* (2007) Rhizobacterial volatile emissions regulate auxin homeostasis and cell expansion in *Arabidopsis*. *Planta*, **226**, 839–851.

Zhang, H.M., Xie, X.T., Kim, M.S., Kornyeyev, D.A., Holaday, S. and Pare, P.W. (2008) Soil bacteria augment *Arabidopsis* photosynthesis by decreasing glucose sensing and abscisic acid levels in planta. *Plant J.* **56**, 264–273.

Zhang, H.M., Sun, Y., Xie, X.T., Kim, M.S., Dowd, S.E. and Pare, P.W. (2009) A soil bacterium regulates plant acquisition of iron via deficiency-inducible mechanisms. *Plant J.* **58**, 568–577.

Zhao, Y. and Hasenstein, K.H. (2010) Physiological interactions of antiauxins with auxin in roots. *J. Plant Physiol.*, **167**, 879–884.

http://doc.rero.ch